High-Resolution Rotational Coherence Spectroscopy of the Phenol Dimer†

Andreas Weichert, Christoph Riehn,* and Bernhard Brutschy

Johann Wolfgang Goethe-Universität Frankfurt/M., Institut für Physikalische und Theoretische Chemie, Marie-Curie-Strasse 11, D-60439 Frankfurt/M., Germany

Received: October 19, 2000; In Final Form: March 26, 2001

We report on an investigation of the phenol dimer by high-resolution rotational coherence spectroscopy (RCS) using the method of time-resolved fluorescence depletion (TRFD). With this technique we determined with high precision the rotational constants of the ground and electronically excited states. The phenol dimer is an ideal model system to study aromatic−aromatic interaction under the constraints of an intermolecular hydrogen bond, which leads to its unique "V-shaped" structure. The TRFD investigation was complemented by an (1 + 1′) pump−probe ionization (PPI) experiment in order to unequivocally assign ground and excited-state transients. Seven different types of RCS transients have been observed in the RCS spectrum and assigned to *H*′′-, *H*′-, *J*′′-, *J*′-, *C*-, *K*-, and *A*-type transients. From a detailed analysis by a grid search procedure based on numerical simulations of RCS spectra and a nonlinear least-squares fitting routine, the following values for the rotational constants have been obtained: $A'' = 1414.4 \pm 0.6$ MHz, $B'' = 313.7 \pm 0.8$ MHz, $C'' = 287.5 \pm 0.7$ MHz, $A' = 1425.7 \pm 2.3$ MHz, $(B' + C') = 590.6 \pm 2.7$ MHz. Furthermore, information about the alignment of the transition dipole moment in the molecular frame was obtained from the fit procedure. We report a geometry of the O−H···O hydrogen bonded phenol dimer as determined by a fit of the intermolecular parameters to the rotational constants. The ground-state results confirm the gross geometry of a former RCS investigation of Felker and co-workers [Connell, L. L.; Ohline, S. M.; Joireman, P. W.; Corcoran, T. C.; Felker, P. M. *J. Chem. Phys.* **1992**, *96*, 2585]. Moreover, it was found that upon electronic excitation of the donor molecule the center of mass distance of the monomer moieties increases slightly from 5.25 Å ± 0.01 Å to 5.31 Å ± 0.05 Å. On the basis of assumptions for structural changes of the hydrogen bond and the donor monomer moiety upon electronic excitation, we propose a modification of the intermolecular structure of the phenol dimer, which is consistent with the experimental data. However, although the changes in the rotational constants are small, larger changes of intermolecular parameters cannot be excluded, e.g., a decrease of the wagging angle by several tens of degrees. The ground-state results are compared with structures obtained from calculations on different levels of theory. In particular, the results from semiempirical calculations based on atom−atom pair potentials and ab initio calculations at the MP2/6-31G(*d*) level of theory are examined.

I. Introduction

The phenol dimer is a prototype molecular cluster system, which has been studied extensively experimentally. The available spectroscopic information unambiguously supports an O−H···O hydrogen bonded dimer structure. However, the relative orientation of the phenyl rings and the contribution of aromatic−aromatic interaction to the intermolecular structure has been debated.[1,2] In particular, up to now no state-selective determination of the rotational constants was available, and especially the structure of the dimer in the electronically excited state is unclear. The landmark study of Felker and co-workers using rotational coherence spectroscopy (RCS) provides the only direct structural results on the phenol dimer, although due to its low time resolution only rotational constants averaged over both electronic states were reported.[1] To determine clearly assigned, state-selective and precise rotational constants for this cluster we started the investigation by high-resolution rotational coherence spectroscopy as described in this account. As a result, we will provide a structural characterization of the phenol dimer for both electronic states. Thus the subtle interplay of hydrogen bonding and aromatic−aromatic dispersion interaction can be followed on a microscopic level.

The first mass-selective electronic absorption spectrum of the phenol dimer was recorded by Fuke and Kaya.[3,4] They assigned the origins of two electronic transitions. One at 36 049 cm^{-1} was assigned to the $S_1 \leftarrow S_0$ transition in the proton donating phenol moiety of a presumed hydrogen bonded dimer, and the second at 36 705 cm^{-1} was assigned to the $S_1 \leftarrow S_0$ transition of the proton accepting moiety. A Raman study performed with ionization loss spectroscopy has been reported by Hartland et al.[5] Dopfer et al. studied the phenol dimer by zero kinetic energy photoelectron spectroscopy and R2PI spectroscopy.[6] Five intermolecular vibrations are observed for the S_1^{donor} state and one for the $S_1^{acceptor}$ state. The ionization energy of the donor was determined to be 63 649 ± 4 cm^{-1}. The ZEKE-PES experiments also suggested that rapid internal conversion between the $S_1^{acceptor}$ and the S_1^{donor} state could exist, which might explain the low fluorescence yield from the $S_1^{acceptor}$ state. The fluorescence lifetime of the donor moiety has been determined by Sur et al.[7] They obtained a lifetime $\tau_e = 16$ ns, with respect to the 2 ns fluorescence lifetime of the phenol

† Part of the special issue "Edward W. Schlag Festschrift".

* To whom correspondence should be addressed. E-mail: riehn@chemie.uni-frankfurt.de.

10.1021/jp003816v CCC: $20.00
Published on Web 05/12/2001

monomer. Ebata et al. performed mass-resolved vibrational spectroscopy of the phenol dimer and trimer.[8] Schmitt et al. studied the UV spectroscopy of the phenol dimer by hole-burning and fluorescence spectroscopy.[9] They were able to rule out the existence of another conformer that absorbs in the spectral region of interest. Four of the six vibrational modes were assigned. Electronic excitation of the donor moiety into the S_1 state leads both to a higher donor acidity and a stronger hydrogen bond (red shift of 304 cm^{-1} of the donor origin with respect to the origin of bare phenol) concomitant with a higher stretch frequency (120 cm^{-1} relative to 109 cm^{-1} in the S_0 state). Apart from the spectroscopic evidence for an O−H···O hydrogen bond, this type of bonding is also energetically favored over, for example, a sandwich-like structure. Typical bond energies are 5 kcal/mol, in contrast to the estimated binding energy of the benzene dimer of about 3 kcal/mol.[1] An ab initio calculation performed at the HF/6-31G(*d*,*p*) level has been reported by Kleinermanns and co-workers,[2,10] showing a hydrogen bonded dimer. Semiempirical calculations based on atom−atom pair potentials including specific hydrogen bond plus extra polarization terms have been performed by Abdoul-Carime et al.[11] Here several conformations with a minimum energy conformation corresponding to the structure of a hydrogen bonded dimer have been reported.

In this work we applied the technique of rotational coherence spectroscopy, which has proved to be a powerful tool for the spectroscopic investigation of large molecules and clusters.[12,13] The phenol donor molecule has been excited in all RCS experiments, because of its higher fluorescence yield as compared to that of the acceptor molecule. Selective fluorescence excitation of the $S_1^{acceptor}$ state (energetically the S_2 state of the molecule) is difficult, because of nearby resonances of the phenol•water cluster and of hot bands. Moreover, it is possible that rapid internal conversion to the S_1^{donor} state occurs.[9] The performed high-resolution time-resolved fluorescence depletion (TRFD) experiments are capable of resolving ground-state and excited-state transients, allowing the determination of the rotational constants of both states.[14] Ancillary state selective RCS methods such as time-resolved stimulated Raman-induced fluorescence depletion (TRSRFD), time-resolved stimulated emission pumping (TRSEP), and (1 + 1′) pump−probe ionization (PPI) are, in particular, useful for the assignment of the different transients to their respective electronic state.[15,16]

The first RCS experiments on the phenol dimer have been performed by Felker and co-workers.[1] A laser pulse width of 30 ps and a total delay range of 2.2 ns was employed to measure the TRFD traces for four isotopomers of the phenol dimer. Four recurrences of hybrid transients and one recurrence of a *J*-type transient have been recorded and identified in the spectrum. Averaged over both electronic states the *A* rotational constant and the sum of $B + C$ has been derived with an estimated uncertainty of 0.5%. The difference $B - C$ has been determined by comparing simulated traces with experimental ones. The relative uncertainty has been estimated to be 50%.

In the following, we report on a new high-resolution RCS experiment, which allowed the precise determination of the three ground-state rotational constants and two parameters of the excited-state rotational constants, based on the assignment of different types of transients and supported by state-selective (1 + 1′) PPI measurements. The results are carefully analyzed to obtain reliable uncertainties and subjected to a thorough sensitivity analysis with respect to the phenol dimer structure. Thus, we propose structures for both electronic states consistent with the experimental results. Moreover, these geometries are cross-checked by ab initio calculations for the ground state.

II. Experimental Setup

A comprehensive description of the experimental setup used for the RCS experiments has been given in previous accounts.[14,17] The main parameters used for the TRFD and the (1 + 1′) PPI experiments are summarized in this section. The RCS spectrometer is based on a solid-state Ti:sapphire laser setup that optically pumps up to two parametric generators (TOPAS) to provide tunable radiation in the UV spectral region. The output parameters of the laser system are: repetition rate 500 Hz, pulse duration 2 ps, bandwidth ≈ 10 cm^{-1}, pulse energy 60 μJ with one TOPAS unit and 2 × 30 μJ with two TOPAS units.

A. Time-Resolved Fluorescence Depletion (TRFD) Experiment. To generate a pump and a probe pulse of the same wavelength, polarization, and energy, the UV radiation of the laser setup was sent through a Michelson interferometer. The probe pulse was delayed in time up to 8 ns by a computer-controlled linear positioning stage. The beams exiting the interferometer were aligned collinearly and focused with a fused silica lens (beam diameter 4 mm, $f = 200$ mm) into a vacuum apparatus. A seeded continuous supersonic expansion (stagnation pressure 2 bar He) was crossed at 2 mm distance from the nozzle (diameter 80 μm). The molecular beam was formed by passing helium over liquid phenol (Fluka, > 99.5% purity) contained in a heated (60 °C) stainless steel container upstream from the nozzle. The nozzle was kept at a slightly higher temperature to prevent condensation of phenol in the orifice. The integral fluorescence was collected by two fused silica lenses, filtered by a long pass filter (Schott, WG295, 2 mm) to reduce stray light, and detected with a photomultiplier tube. The fluorescence signal was recorded with a boxcar integrator. A chopper, synchronized to half the repetition rate of the laser system, was employed in the fixed arm of the interferometer[17] to perform ON/OFF measurements in the manner of a digital lock-in technique. With the laser running at a repetition rate of 500 Hz, these data were digitized by an ADC card, averaged over 500 events per delay line and chopper setting, and stored in a personal computer. The whole delay range has been divided into 32 sections that have been scanned separately with a step size of 1.5 ps. Each section has been scanned 20 times in alternating directions (2 × 10 scans). Regions with special importance for the assignment of certain transients have been scanned more often. Features with modulation intensities < 0.1% have been clearly identified and resolved. A total data acquisition time of more than 120 h was necessary for recording the TRFD spectrum with the obtained *S*/*N* ratio. The first hybrid transient at ≈447 ps was recorded before each measurement to ensure a constant quality of the experimental conditions. This transient was optimized on all days of measurement within tight tolerances (<10%) with respect to its absolute modulation intensity and its width. The positional accuracy of the time zero of the interferometer is estimated to be better than 100 fs for the whole measurement. It was calibrated by using a nonlinear effect in a silicon photodiode.[17]

B. (1 + 1′) Pump−Probe Ionization (PPI) Experiment. A two-color pump−probe setup has been used for the (1 + 1′) pump−probe ionization (PPI) experiments.[16,17] The frequency for the pump pulse was adjusted to excite the origin of the donor moiety while that of the probe pulse was red shifted by 150 cm^{-1}. The probe pulse was out of resonance with any molecular transitions in the neutral manifold. The pulse energy of the

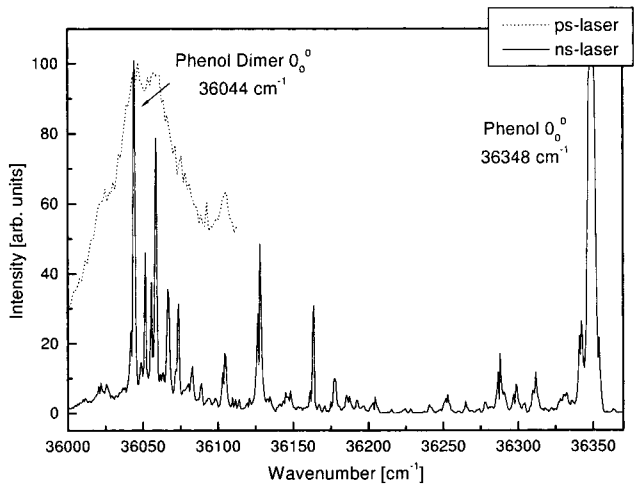

Figure 1. LIF spectrum of a supersonic expansion of phenol in the vicinity of the 0_0^0 transition of the phenol dimer. The spectrum measured with the picosecond laser was obtained under typical conditions of an RCS measurement. Assignments taken from ref 8.

resonant pump pulse was attenuated to 1/5 of the pulse energy of the probe pulse in order to minimize the signal due to one-color R2PI. Pump and probe pulse were recombined on a dielectric 50/50 beam splitter and focused into the ionization region of a time-of-flight mass spectrometer by a $f = 100$ mm or a $f = 150$ mm fused silica lens. A home-built Wiley−McLaren-type time-of-flight mass spectrometer ($m/\Delta m \approx 300$) was used for the detection of the ions at the mass of the phenol dimer (188 amu). The ionization region was located approximately 10 cm downstream of the nozzle in a differentially pumped ionization chamber. To measure transients in the (1 + 1′) ion yield, especially the spectral section around the second recurrence of the *J*-type transient has been scanned more than 100 times in alternating directions.

III. Experimental Results

Figure 1 shows a fluorescence excitation spectrum of a supersonic expansion of phenol in the vicinity of the 0_0^0 transition of the phenol dimer, i.e., of the origin of the phenol donor moiety. The scan with the picosecond laser has been obtained under RCS measurement conditions, showing a strong saturation, which was necessary to produce RCS recurrences. However, the picosecond laser with a bandwidth of $\approx$10 cm^{-1} was carefully adjusted on the low energy edge of the 0_0^0 transition by comparison with a high-resolution scan with a ns laser (Figure 1). Due to the strong dependence of the RCS− modulation intensity on the saturation of the 0_0^0 transition, it can be concluded that other, weaker transitions, do not produce noticeable modulations in the RCS trace of this system.

A. TRFD Experiment. Figure 2 provides an overview of the TRFD RCS trace of the phenol dimer, measured up to a delay time of 7.2 ns. Care has been taken in merging the raw data trace from 32 partially overlapping segments. A mathematical high-pass filter with a time constant of 150 ps was employed to eliminate a long-term curvature of the signal. For the presentation of the experimental spectrum, a smoothing of the raw data with 7.5 ps adjacent averaging was employed.

Hybrid-type (*H*-type) and *J*-type transients are easily identified in the spectrum because of their alternating polarity.[13] They can be distinguished by their intensity variation. Thus, positive and negative recurrences of *H*-type transients have the same modulation intensity, whereas the positive recurrences of *J*-type transients show a lower intensity than the negative recurrences.[18] A splitting of the *H*-type transients was observed starting with the fourth recurrence at 1780 ps. There is also evidence for a splitting of the *J*-type transients starting with the second recurrence at 1675 ps, which has been confirmed and assigned by the (1 + 1′) PPI experiment, as discussed in the next section. *K*-type recurrences are expected with negative polarity at half the recurrence time of the *H*-type transients. The first recurrence of this type can be seen clearly in the simulation and the experimental trace at 223 ps. This feature, and its relative modulation intensity, has been confirmed by several scans. *C*-type asymmetry transients are expected to arise for asymmetric prolate tops.[13] *A*-type recurrences are expected because of the hybrid type of the transition dipole moment. The intensity, polarity, and shape for these transients are not as strictly defined as for the other types of transients and may vary through an RCS spectrum. The second recurrence of an *A*-type transient

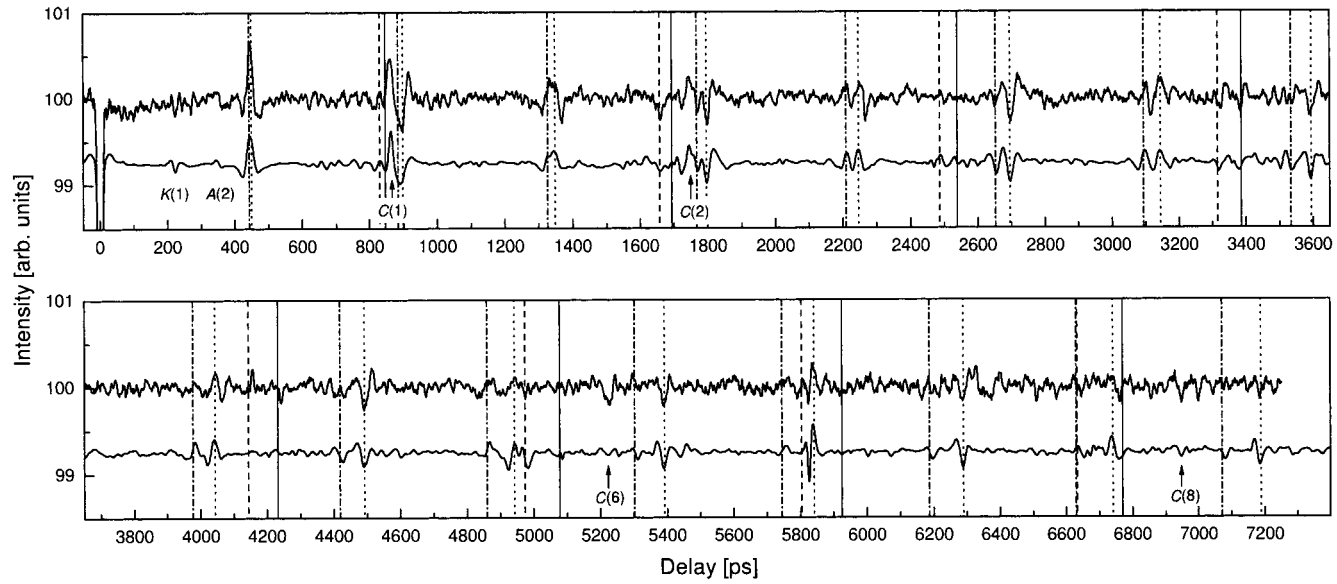

Figure 2. TRFD RCS overview spectrum of the phenol dimer. The upper trace represents the experimental data and the lower trace the simulation. Four different types of transients are identified, and their positions are marked by vertical lines: *H*″, dotted; *H*′, dashed−dotted; *J*″, dashed; and *J*′, full line. The positions of some *K*-, *A*-, and *C*-type transients are also indicated in the spectrum.

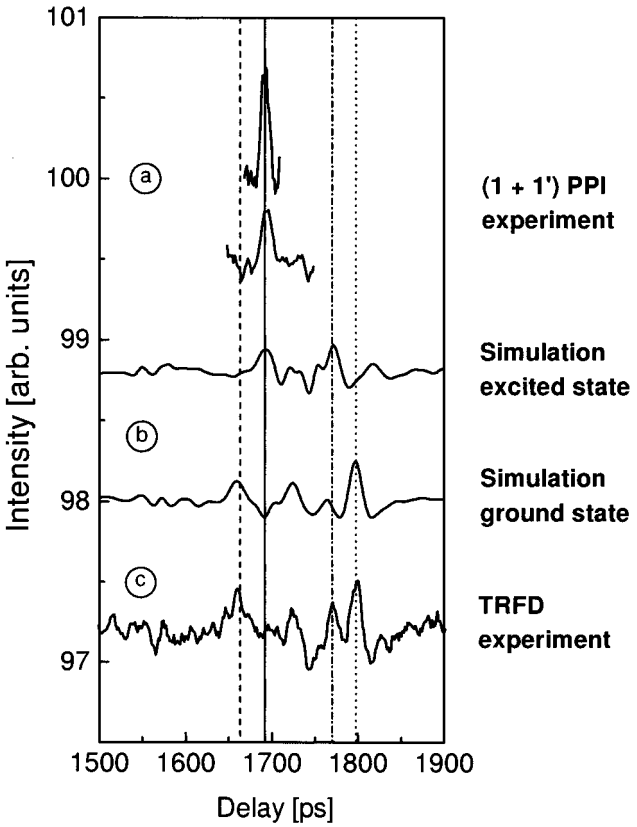

Figure 3. (1 + 1′) PPI RCS spectrum in the region of the second recurrence of the *J*-type transients. Simulations of the electronic ground state and the excited state are shown for comparison. The simulations and the experimental TRFD trace are plotted with inverted polarity.

can be seen at ≈353 ps. Modulations caused by *C*-type transients are indicated in the spectrum at ≈870 and ≈1740 ps. Special interest was caused by the strong feature at ≈5224 ps in the experimental trace, which could be explained by the sixth recurrence of a *C*-type transient of the ground state. Another *C*-type recurrence, which is consistent with this assumption, is also marked in the spectrum at ≈6965 ps. A simulated spectrum, representing the best fit to the data, is shown below the experimental trace for comparison.

B. (1 + 1′) PPI Experiment. The applicability of the (1 + 1′) PPI method has been demonstrated for the first time by recording an RCS spectrum of *para*-cyclohexylaniline.[16] This method proved very sensitive for the *J*-type transients of the electronically excited state of this system. Figure 3 shows the (1 + 1′) PPI RCS trace obtained in the region of the second recurrence of the *J*-type transients of the phenol dimer. The data of the experimental TRFD spectrum and a simulated spectrum for the ground state and the excited state are given for comparison. Note that the simulated traces and the experimental TRFD spectrum are shown with inverted polarity to allow a better association with the (1 + 1′) PPI experiment.

IV. Computational Results for the Phenol Dimer

Using the GAUSSIAN 94 package[19] we performed both ab initio calculations at the MP2 level of theory, which includes first-order electron correlation, and calculations at the HF and DFT/B3LYP level. For all calculations the 6-31G(*d*) basis set has been used, consisting of 234 basis functions for the phenol dimer. A full geometry optimization was carried out applying the standard convergence criteria. C_1 symmetry was found. The MP2 calculations have been performed with two different start

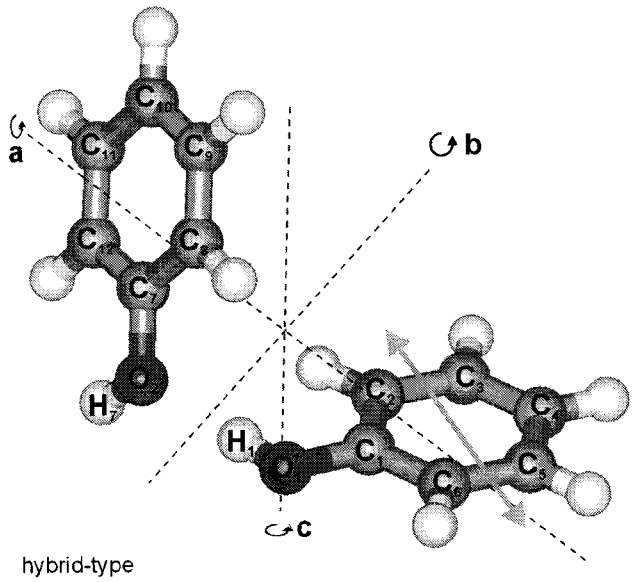

Figure 4. Structure of the phenol dimer in the electronic ground state (S_0). The atom numbering system used to define the internal coordinates of the phenol dimer has been adopted from ref 1. The molecular axis system was assigned according to Mulliken.

geometries, which converged to the same final structure. The first start geometry was the result of an ab initio calculation at the HF level performed by Kleinermanns and co-workers,[2,10] and the second was the result of a semiempirical calculation reported by Abdoul-Carime et al.[11] Both calculations are introduced below, and characteristic parameters are given in Table 4. The resulting structure, obtained after full geometry optimization, is depicted in Figure 4. The intermolecular parameters that characterize this structure are listed in Table 4. The results are in good agreement with the experimentally obtained rotational constants of the phenol dimer. The differences between the calculated and measured *A*, *B*, and *C* rotational constants are 3.5%, 3.7%, and 6.3% respectively. The rotational constants obtained for the donor and acceptor moiety are close to the experimental values of bare phenol. The distance between the CM of both phenol moieties is 5.097 Å, and the wagging angle $\angle\, C_1O_1O_2C_7$ (see Figure 4) has been found to be −69.6°.

Semiempirical calculations on the phenol dimer using the MINGEN program have been reported by Abdoul-Carime et al.[11] Several possible structures have been found by applying a genetic algorithm for the global energy minimum search, but the absolute minimum energy structure corresponded to a hydrogen-bonded dimer with a geometry close to the structure obtained at the MP2 level. Its rotational constants were very similar to the experimental values (see Table 4).

The successful application of ab initio calculations at the MP2 level of theory and additional force field calculations helped to elucidate the structure of the naphthalene trimer, as reported recently. Following an experimental RCS study of the naphthalene trimer performed by Benharash et al.,[20] an ab initio investigation of this species was performed by Gonzalez and Lim.[21] The experimentally found rotational constants were in good agreement with the minimum energy structure of ab initio calculations at the MP2/6-31G level of theory. A very similar structure has been found by less expensive force field calculations at the MM3 level. We think that the success of both theoretical approaches in determining the gross geometry

TABLE 1: Summary of Experimental and Theoretical Rotational Constants and Related Data of the Phenol Dimer

		TRFD RCS				
	linear regression	set I $t_H'' > t_H'$	set II $t_H'' < t_H'$	former RCS expt. [ref 1][a]	semi-emp. calculation [ref 11]	ab initio calc [this work][b]
			Recurrence Times (ps)			
t_H''	449.2(1)	448.91 ± 0.2	442.33	446.8 ± 2.2	479.6	475.8
t_H'	442.5(2)	442.33 ± 0.7	448.91			
$(t_H' - t_H'')/t_H''$	−1.5 %	−1.5 %	1.5 %			
t_J''	829.5(4)	831.74 ± 0.8	831.74	834.7 ± 4.2	828.9	792.3
t_J'	844.8(6)	846.71 ± 3.8	846.71			
$(t_J' - t_J'')/t_J''$	1.8%	1.8 %	1.8 %			
			Rotational Constants (MHz)			
A''	1414.5(3)	1414.4 ± 0.6	1431.0	1418.6 ± 5.7	1344.1	1366.4
B''		313.7 ± 0.8	313.7	313.5 ± 14	318.0	325.6
C''		287.5 ± 0.7	287.5	285.5 ± 14	285.2	305.5
$B'' + C''$	602.5(3)[c]	601.2 ± 0.6	601.2	599.0 ± 3.0	603.2	631.1
A'	1425.9(6)	1425.7 ± 2.3	1409.1			
B'		315.3 ± 7.9	315.3			
C'		275.3 ± 6.9	275.3			
$B' + C'$	591.6(5)[c]	590.6 ± 2.7	590.6			
κ''		−0.9535	−0.9542	−0.9506	−0.9380	−0.9621
κ'		−0.9305	−0.9294			
b_p''		−0.012	−0.012	−0.013	−0.016	−0.010
b_p'		−0.018	−0.018			
			Alignment of TM (%)			
a		53.4	53.4	51.7	55.5	44.4
b		31.2	31.2		13.7	3.4
c		15.4	15.4		30.8	52.1

[a] The values have to be considered as averaged over the ground state and the electronically excited state rotational constants. [b] MP2/6-31G(*d*) level of theory. [c] Including the b_p asymmetry correction factor (see ref 13).

of large clusters is very encouraging for theoretical calculations for other systems.

HF and DFT/B3LYP ab initio calculations are known to underestimate the dispersive interaction caused by electron correlation, which is not included on the HF and not well described on the DFT/B3LYP level. It is therefore not unexpected that the geometries obtained by these methods are different. The CM distances are 6 and 5.9 Å, and the wagging angle $\angle$ $C_1O_1O_2C_7$ is −108° and −110°, respectively. One ab initio calculation on the phenol dimer has been reported in the literature.[2,10] The calculation has been performed at the HF/6-31G(*d,p*) level of theory and reveals the typical deficiencies for this level of theory. A hydrogen bonded dimer was found, with a typical $O_1 - O_2$ distance of 2.97 Å and an oxygen atom O_2 that is shifted by ≈0.1 Å out of the plane defined by the phenol donor moiety ($\angle$ $C_2C_1O_1O_2 = -2.1°$). The largest difference in comparison with the MP2 S_0 structure is the wagging angle $\angle$ $C_1O_1O_2C_7$ of −107.5°, in comparison to −69.6° for the MP2 calculation. This results in a large CM distance of 6 Å and an *A* rotational constant that is ≈420 MHz larger than the experimental value.

V. Analysis of Experimental Results

To obtain the rotational constants of the ground state and the electronically excited state, two methods of analysis for the recorded RCS spectra have been employed. The first was a linear regression analysis of transient peak positions assuming a nearly symmetric prolate top. In a second approach numerical simulations of the full RCS spectra were employed and fitted to the experimental data. Before those methods can be applied, the transients of the ground state and the electronically excited state have to be distinguished.

A. Assignment of Ground-State and Excited-State Transients. The results of the (1 + 1′) PPI experiment are used to assign the excited-state *J*-type transients. There is a transient with a positive polarity that corresponds to the assumed position of an excited state *J*-type transient. Therefore, it can be concluded that $t_J'' < t_J'$. The polarity of this transient is inverted with respect to the TRFD trace, which can be rationalized because of a gain process in the (1 + 1′) PPI scheme instead of a depletion process in the TRFD scheme. This observation is in agreement with the polarity of the (1 + 1′) PPI data obtained on *J*-type transients of *p*CHA[16,22] and on *J*-type transients of *p*DFB•Ar.[23,24]

An assignment of the *H*-type transients to ground-state and electronically excited-state transients has been done on the basis of a comparison with simulated spectra. Two alternative assignments $t_H'' > t_H'$ (set I) and $t_H'' < t_H'$ (set II) have been compared (see Table 1). Figure 5 shows five regions around the positions of the *H*-type transients, which have been selected because they show a significant difference between the simulation of set I and the simulation of set II. The better agreement of simulation I with the experimental data leads to the assignment $t_H'' > t_H'$, which has been assumed for further analysis.

B. Linear Regression Analysis. The peak positions were extracted for the *H*″-, *H*′-, *J*″-, and some *J*′-type transients. With these data a linear regression analysis was performed [Figure 6a]. The residuals are depicted in Figure 6b, which reveals a variation in the measured positions from a straight line fit by less than ±5 ps. As a result of this procedure, the following algebraic relations have been obtained for the rotational constants:

$$t_H'' = 1/[2\ A - (B + C)]'' = 449.2(1)\ \text{ps} \quad (1)$$

$$t_H' = 1/[2\ A - (B + C)]' = 442.5(2)\ \text{ps} \quad (2)$$

$$t_J'' = 1/(B + C)'' = 829.5(4)\ \text{ps} \quad (3)$$

$$t_J' = 1/(B + C)' = 844.8(6)\ \text{ps} \quad (4)$$

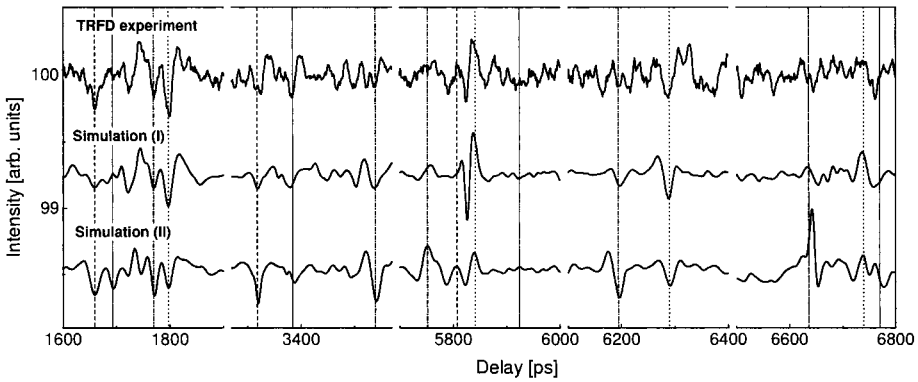

Figure 5. Magnified regions of the TRFD RCS spectrum of the phenol dimer. Comparison of the experimental trace with the two possibilities in the assignment of the *H*-type transients with respect to the ground state and the electronic excited state. Simulation (I), $t_H'' > t_H'$; simulation (II), $t_H'' < t_H'$.

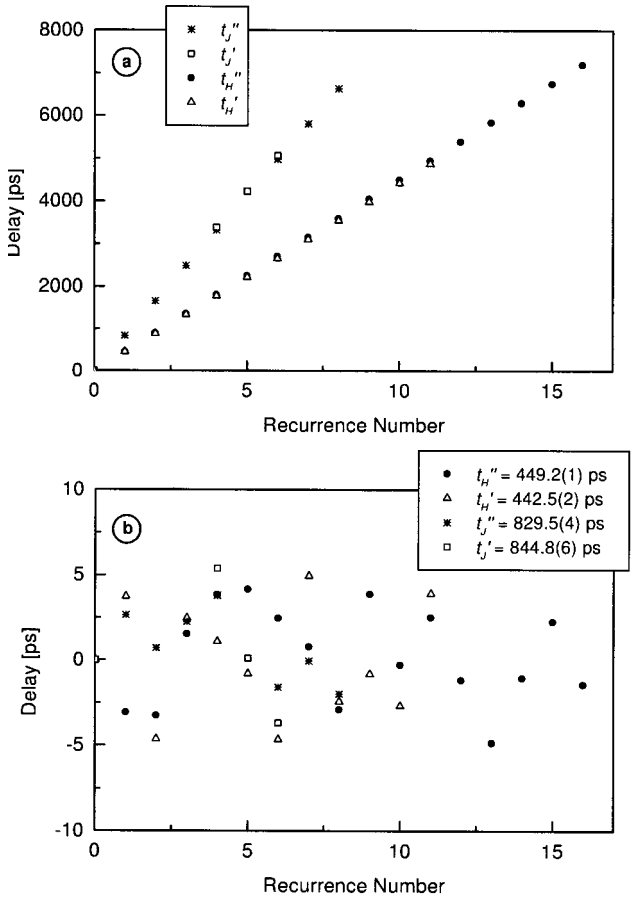

Figure 6. Linear regression analysis of the RCS spectrum of the phenol dimer. Evaluation of *H*″-, *H*′-, *J*″-, and *J*′-type transients. (a) Straight line fit. Plot of delay time vs recurrence number *n* for the measured and identified transients. (b) Regression residua.

The error margins correspond to the statistical error of the linear regression procedure assuming an experimental uncertainty in the peak positions of 3 ps for the *H*″-type transients, 3−5 ps for the *H*′-type transients, and 5 ps for the *J*″- and the *J*′-type transients. From these data the following rotational constants were calculated: $A'' = 1414.5 \pm 0.6$ MHz (0.04%), $(B + C)'' = 602.5 \pm 0.6$ MHz (0.1%), $A' = 1425.9 \pm 1.2$ MHz (0.08%), $(B + C)' = 591.6 \pm 1$ MHz (0.2%). The reported uncertainties correspond to 2σ (standard deviation), relative uncertainties are given in parentheses. The difference between *B* and *C* reflects the asymmetry of the cluster. It cannot be obtained from the linear regression approach, but only by using additional information. This information can be obtained from the positions of *C*-type recurrences and by comparing the relative modulation intensities of different types of transients, together with a fit of a simulated spectrum to the experimental data.

C. Simulation and Fit of RCS Spectra. The methodology used to fit simulated spectra to the experimental data has been described in detail in a previous publication on *para*-cyclohexylaniline.[14,25] The input parameters for the search and fit procedure were the rotational constants, the alignment of the transition dipole moment (TM) within the molecular frame, the rotational temperature of the sample T_{rot}, the pulse duration of the laser τ_{laser}, and the fluorescence lifetime of the excited state τ_e. Additionally, a scaling factor (SF) for the intensity of the depletion and an offset parameter are fitted. Starting with the rotational constants obtained from the linear regression analysis, a two-dimensional search for the alignment of the transition dipole moment has been performed. The fluorescence lifetime τ_e was fixed to 16 ns[7] and a laser pulse duration of $\tau_{laser} = 2$ ps was assumed. The optimized alignment of the TM has been used as a starting point for a refinement of the rotational constants by a Levenberg−Marquardt algorithm[26] to fit the simulation to the experimental TRFD trace. Both procedures were repeated iteratively several times.

Instead of fitting the rotational constants (*A*, *B*, *C*) directly, a different set of coordinates (t_H, t_J, *C*) was used. This has the advantage that all coordinates refer directly to distinct observable transients in the spectrum and are therefore uncorrelated. The transformation between these two sets of coordinates is

$$A = {}^1/_2\,[1/t_H + 1/(2\,t_J)]$$
$$B = 1/(2\,t_J) - C \qquad (5)$$

A grid search routine together with a nonlinear fitting routine was used to find optimized sets of parameters. The results for the best fit obtained are given in Table 1 (set I). The error margins were obtained by variation of one parameter and subsequent optimization of the others.[14] The results of the search and fit procedure, which are relevant to the error analysis, are depicted in Figure 7. The reduced χ^2 was calculated with and without relaxation of the remaining fit parameters. The $\Delta\chi^2/\chi^2_{min} = 2\%$ boundary is indicated as a horizontal line and the value for the corresponding relative uncertainty is given in each plot.[27] Note that the ground-state parameters were given with high accuracy, in particular the transient times t_H'' and t_J'' connected with A'' and $(B + C)''$, respectively. Also C'', which is linked to the difference $(B - C)''$, was determined accurately. The situation was different for the excited-state parameters t_J' and C' (note the different scaling of the *x*-axis). This is due to

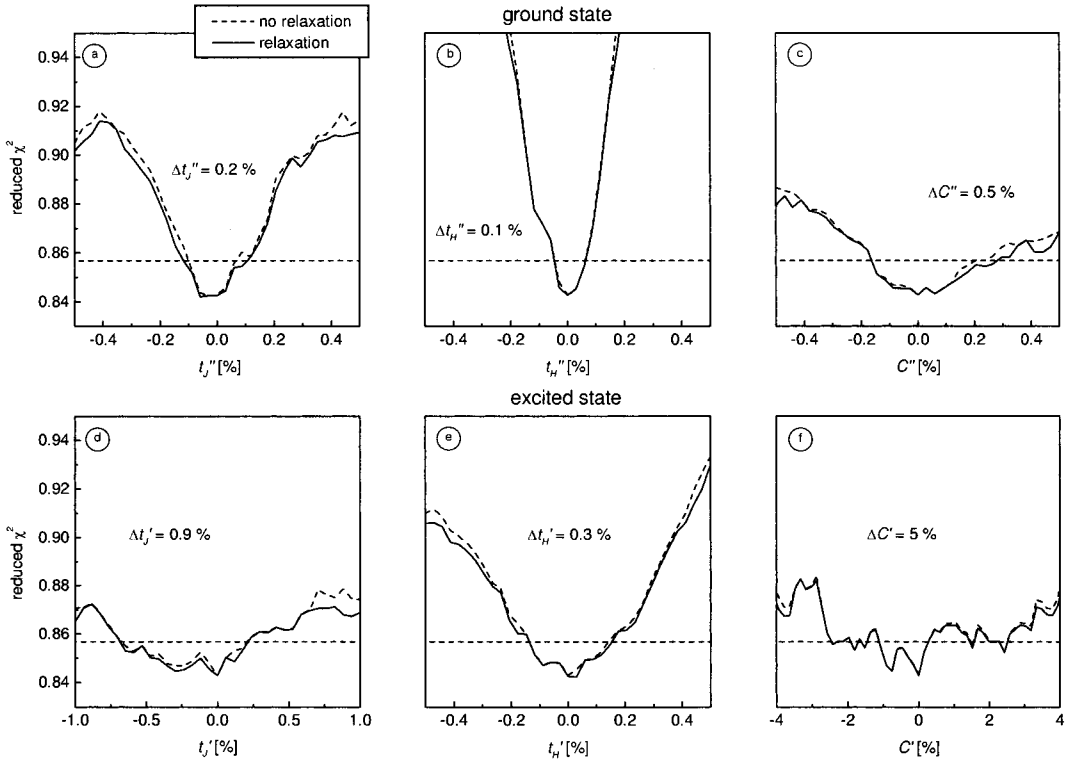

Figure 7. Error analysis for the adapted parameters (t_H, t_J, C). The neighborhood of an optimized set of rotational constants obtained from the Levenberg−Marquard procedure as investigated by a grid search and grid search with relaxation method. The reduced χ^2 is plotted as a function of the variation of the fit parameters relative to their minimum value. $\Delta\chi^2$ boundaries that correspond to a high level of confidence ($> 2\sigma$) are indicated ($\Delta\chi^2/\chi^2_{min} = 2\%$) by the dashed horizontal lines. The corresponding value is given in each plot.

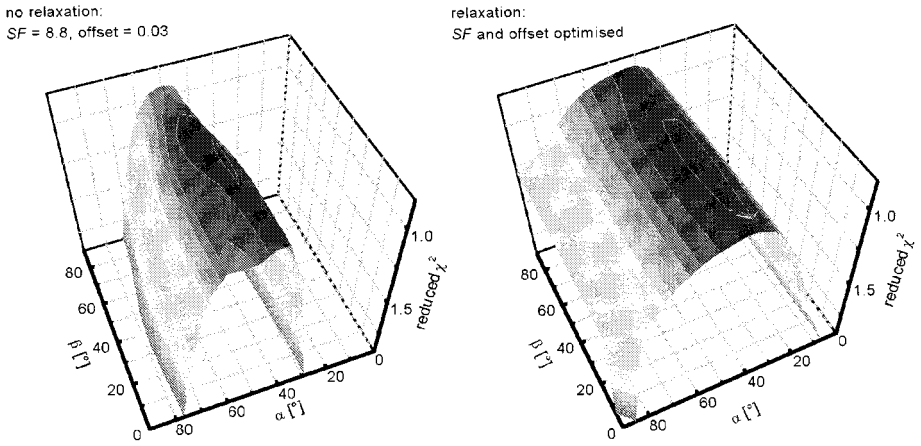

Figure 8. Variation of the reduced χ^2 by changing the alignment of the transition dipole moment (TM): (a) $\chi^2(\alpha, \beta)$ without relaxation of the other parameters; (b) $\chi^2(\alpha, \beta)$ with relaxation of the scaling factor SF and the offset parameter.

the fact that the J'-type transients are very weak in the TRFD trace and that no clearly visible excited state C-type transients have been identified. Hence, the relative uncertainty for $(B - C)'$ is 40%, in comparison with only 4% for $(B - C)''$. The results of the error analysis are summarized in Table 1.

The optimized values of the rotational constants have been used to perform a two-dimensional fit concerning the alignment of the transition dipole moment (TM).[28] Figure 8 shows the dependence of $\chi^2(\alpha, \beta)$ for the optimized set of rotational constants. α refers to the angle between the TM and the a axis, and β is the angle in the b/c plane with respect to the b axis. The scaling factor SF and the offset parameter are optimized in the relaxed plot. A sensitive dependence of χ^2 on the angle α and a less sensitive dependence of χ^2 on the angle β was found. The optimum values are $\alpha = 43^{+12°}_{-8°}$, $\beta \approx 35°$, and SF = 8.5 (Figure 8). The differences in the simulated spectra on varying α can be described as follows. The decrease of α leads to stronger J-type transients in comparison with the H-type transients. An increase leads to stronger A- and K-type transients. The boundaries for α have been determined in comparison with the relative modulation intensities of those transients in the experimental TRFD spectrum.

In Figure 9 the results obtained by variation of the lifetimes for the ground state (τ_g) and the excited state (τ_e) are depicted. The curves have been obtained by optimizing the parameters SF and offset. $\chi^2(\tau_e)$ shows a minimum for $\tau_e = 17^{+55}_{-10}$ ns, whereas $\chi^2(\tau_g)$ reaches its minimum for $\tau_g \rightarrow \infty$. These observations confirm the assignment of ground-state and excited-state transients. The result for the lifetime τ_e is also consistent with a value of $\tau_e = 16$ ns, as reported in ref 7.

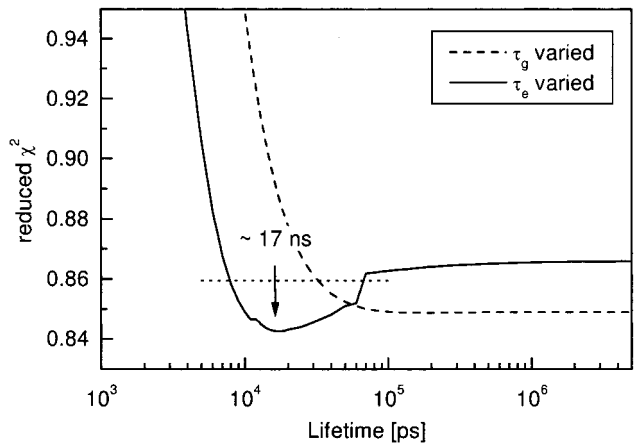

Figure 9. Change of the reduced χ^2 upon variation of the fluorescence lifetime for the ground state (τ_g) and the excited state (τ_e) in the simulated spectrum.

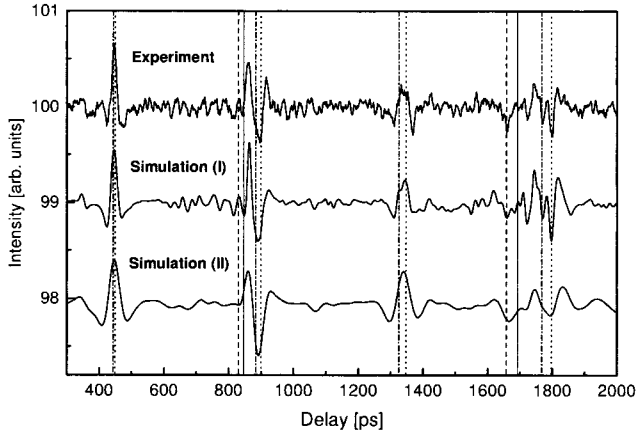

Figure 10. Comparison of the high-resolution experimental data of this work with two simulations. Simulation (I) (τ_{laser} = 2 ps, T_{rot} = 8 K), corresponds to the experimental parameters of this work, and simulation (II) (τ_{laser} = 30 ps, T_{rot} = 5 K) corresponds to a simulation of the TRFD experiment of Felker and co-workers.[1] The positions of four different types of transients are marked by vertical lines: *H*″, dotted; *H*′, dashed−dotted; *J*″, dashed; and *J*′, full line.

D. Comparison with Former Experimental Results. The results of the former RCS study of Felker and co-workers[1] on the hydrogenated phenol dimer are compared in Table 1 with the results of our high-resolution study. The reported rotational constants are in good agreement with the averaged values obtained from evaluation of the ground-state and the electronic excited-state transients. The simulated spectra, corresponding to different measurement conditions, are compared in Figure 10. We used the parameters τ_{laser} = 2 ps and T_{rot} = 8 K for our study (simulation I), and τ_{laser} = 30 ps and T_{rot} = 5 K for the former RCS investigation[1] (simulation II). The rotational constants have been taken from the best fit to the high-resolution experimental data (see Table 1, set I). The depicted time delay range corresponds to that of Figure 5 in ref 1. Four recurrences of *H*-type transients and two recurrences of *J*-type transients are observed. A splitting of the transients into ground-state and excited-state transients is observable both in the experimental trace and in simulation (I) but not in the depicted part of simulation (II). This can be explained by the fact, that only the average rotational constants have been obtained in the former TRFD study. The alignment of the transition dipole moment, extracted in the former RCS investigation, was characterized by $\alpha \approx 44°$, which is in very good agreement with $\alpha \approx 43°$ obtained by the two-dimensional fit to our data (see Figure 8). The averaged difference $B - C$ that has been extracted was 28 MHz, in agreement with a value of 33 MHz obtained for $[(B - C)'' + (B - C)']/2$ from the data of this work.

VI. Structural Analysis

A. Phenol Monomer Geometry. The phenol monomer has been studied intensively both experimentally and theoretically. Larson obtained precise rotational constants from microwave spectra. He also deduced a complete substitution structure by measuring the isotopomers and applying the Kraitchman equations.[29,30] However, the substitution structure r_s does not represent a zero-point energy structure r_0, and therefore the rotational constants from the r_s structure are slightly different from the microwave data. The rotational constants of the electronically excited state have been reported by Hollas et al. by measuring and evaluating a rotational band contour of phenol[31] (see ref 32 for a review). Berden et al. applied high-resolution UV spectroscopy to derive the ground-state and excited-state rotational constants of bare phenol and the phenol•water cluster.[33] A crystal structure analysis of phenol by X-ray diffraction has been reported by Zarodnik et al.[34] Three slightly different structures have been obtained because of a helical structure in the crystal, with three phenol molecules per turn. An electron diffraction study has been performed by Hargittai and co-workers.[35] Ab initio calculations for bare phenol have been performed at various levels of theory. See, for example, the work of Lampert et al., Michalska et al., Fang, and Roth et al.[36−39] Calculations at the MP2/6-31G(*d*,*p*) and DFT/B3LYP/6-31G(*d*,*p*) levels of theory reproduced the rotational constants of the ground state quite well,[36,37] whereas CAS(8,7)/6-31G(*d*,*p*) calculations, with an active space of eight electrons and seven orbitals, had to be employed to give a good description of the excited-state rotational constants.[37,38] Table 2 summarizes some of the rotational constants of the phenol monomer, which are reported in the cited publications.

B. Phenol Dimer Geometry. Several assumptions have to be made in order to derive effective zero-point energy structural information from the rotational constants obtained for the phenol dimer. Following the analysis of Felker and co-workers,[1] the distance *R* between the two centers of mass of both monomers can be expressed as

$$\mu R^2 = \frac{1}{2}\left(\sum_x I_x^{(D)} - \sum_x I_x^{(1)} - \sum_x I_x^{(2)}\right) \tag{6}$$

$$\mu = \frac{m_1 m_2}{m_1 + m_2} \tag{7}$$

where μ is the reduced mass of both monomers, and I_x are the principle moments or inertia of the dimer $I^{(D)}$, monomer one $I^{(1)}$, and monomer two $I^{(2)}$. The individual moments of inertia are connected to the rotational constants by

$$I_x = \frac{h}{8\pi^2 X} \qquad X = A, B, C \tag{8}$$

Because eq 6 is a general result, assumptions about the geometry of the monomer moieties have to be put forward in order to calculate the intermolecular distance *R*.

The rotational constants obtained from Berden et al. have been used for the calculation of the intermolecular CM distance *R* of the phenol dimer (equations 6−8). The ground-state rotational constants of bare phenol have been assumed for both

TABLE 2: Rotational Constants (MHz) of Bare Phenol Obtained by Different Methods

	microwave spectroscopy (r_0)[29]	microwave spectroscopy (r_s)[a]	rotational contour analysis[41]	UV spectroscopy[33]	electron diffraction[35]	X-ray diffraction[b]	ab initio calculations[c]	ab initio calc[d]
A''	5650.5154(11)	5667.8	5650.49	5650.515(6)	5610	5802	5674.6	5650.6
B''	2619.2360(5)	2625.6	2619.29	2619.236(3)	2628	2674	2619.2	2614.6
C''	1789.8520(3)	1794.4	1789.76	1789.855(3)	1789	1831	1789.9	1787.5
A'			5315.3 ± 6	5313.6(2)			5352.1	
B'			2623.5 ± 1.8	2620.5(1)			2576.9	
C'			1756.5 ± 0.3	1756.10(4)			1739.4	

[a] Calculated from the structural parameters deduced in ref 29. [b] Average values of the three species.[34] [c] CAS(8,7)/6-31G(*d*,*p*) level.[37] [d] MP2/6-31G(*d*,*p*) level.[37]

phenol moieties to calculate R'' of the dimer. For the electronically excited state we assumed the rotational constants of the molecular excited state for the donor moiety and that of the ground state for the acceptor moiety to calculate R'. The results are $R'' = 5.255$ Å $\pm$ 0.005 Å, $R' = 5.311$ Å $\pm$ 0.04 Å, and $(R'' + R')/2 = 5.28$ Å. The average value is in good agreement with the value of $R = 5.27$ Å obtained by Felker and co-workers.[1]

To derive structural information for the phenol dimer from the RCS results, the assumption has been made that the monomer geometries do not change upon complexation. The MP2 ab initio calculations show that this assumption is justified for the electronic ground state. There are six independent intermolecular coordinates that have to be determined in order to characterize the intermolecular structure of the phenol dimer. These are the three components of the distance vector $\boldsymbol{R}$ connecting the centers of mass of both monomers and the three Euler angles (ϕ, θ, χ).

The values for the three rotational constants of the dimer have been obtained from the experimental data. However, for an unequivocal determination of the six intermolecular coordinates, which determine the intermolecular structure, at least three more constraints are necessary. The geometrical results of the following constraints have been tested: (i) We assumed an O−H···O hydrogen-bonded dimer with a linear O−H···O bond, which corresponds to an in-plane bend angle $\angle\ C_1O_1O_2 = 108.8°$ and an out-of-plane bend angle $\angle\ C_2C_1O_1O_2 = 0°$. Additionally an O_1-O_2 distance of 3.00 Å has been assumed. The first two assumptions have also been made by Felker and co-workers.[1] The value for the O_1-O_2 distance was assumed according to the fitting results of reference 1. (ii) $\angle\ C_1O_1O_2 = 108.8°$, $\angle\ C_2C_1O_1O_2 = 0°$, and an O_1-O_2 distance of 2.93 Å (value from the phenol•water cluster[33]). (iii) $\angle\ C_1O_1O_2 = 108.8°$, $\angle\ C_2C_1O_1O_2 = 0°$, and an alignment angle of the transition dipole moment (TM) of $\alpha = 43°$, as determined from the fit to the TRFD spectrum.[40]

The procedure of the structural analysis was as follows: First a dimer is constructed using the structure of two phenol monomer moieties, with the six intermolecular coordinates determining their relative orientation. Then the rotational constants of the dimer and other intermolecular parameters of interest (e.g., O_1-O_2 distance, $\angle\ C_1O_1O_2$, $\angle\ C_2C_1O_1O_2$, α, β, ...) are calculated. To fit the six intermolecular coordinates to the constraints of the phenol dimer, a nonlinear fitting routine based on a Levenberg−Marquardt algorithm[26] has been employed.

The phenol monomer geometries, used for the fit procedure, have been constructed to fit the measured rotational constants of the phenol monomer. The method, that has been suggested by Cvitaš et al. and Berden et al., has been employed.[41,33] The chosen characteristic ground-state and excited-state parameters used for the construction of the phenol dimer are given in Table 3. As pointed out by Berden et al., neither the monomer geometry nor the structural changes upon electronic excitation are unambiguous. The structures are merely an example of structures that are consistent with the rotational constants.

TABLE 3: Structural Parameters Used for the Phenol Moieties in the S_0 and S_1 State (Constructed as Described in the Text) Compared with the Values of the Substitution Structure[29]

	microwave (r_s)[29]	S_0	S_1
Structural Parameters [Å, °]			
C_1-O	1.375	1.3745	1.2564
C_1-C_2, C_3-C_4, C_4-C_5, C_6-C_1[a]	1.393	1.3956	1.4439
C_2-C_3, C_5-C_6[a]	1.393	1.3956	1.443
$C-H$[a]	1.083	1.084	1.084
C_2-H_2	1.0856	1.0856	1.0856
$O-H_1$	0.957	0.9574	0.9574
$\angle\ C_6C_1C_2$	120.9	120.9	120.9
$\angle\ C_2C_3C_4$	120.5	120.5	120.5
$\angle\ C_4C_5C_6$	120.8	121.1	121.1
$\angle\ C_1C_2C_3$	119.4	119.4	119.4
$\angle\ C_3C_4C_5$	119.2	119.2	119.2
$\angle\ C_5C_6C_1$	119.2	118.9	118.9
$\angle\ C_1O_1H_1$	108.8	108.8	108.8
Rotational Constants [MHz]			
A	5667.8	5650.1	5313.7
B	2625.6	2620.2	2621.0
C	1794.4	1790.1	1755.2

[a] Average values.

The results of a fit to the above three exemplary boundary conditions are given in Tables 4 and 6. As can be seen from Table 4, structure (I) is very similar to the structure reported by Felker and co-workers. Structure (II) exhibits only minor modifications of some angles, whereas structure (III) shows stronger deviations. Because of the large uncertainty of α ($^{+12°}_{-8°}$), this structure, which has been determined with α and the constraint of a linear hydrogen bond, is thought to be less reliable. Structures (I) and (II) are thought to be a good representation for the electronic ground state of the phenol dimer. Moreover, the intermolecular parameters are in good agreement with the structure obtained from the MP2 ab initio calculations.

As a test of the proposed structure (I), we compared it with the results of the experiments on the deuterated species performed by Felker and co-workers.[1] In their RCS study, four different phenol dimer isotopomers, i.e., h_6-h_6, d_1-d_1, d_6-d_6, and d_5-d_5, were investigated. Four sets of rotational constants have been determined, and four values of R have been evaluated by assuming that the structure of the phenol dimer is not changed upon deuteration. Felker and co-workers obtained their structure by fitting all deuterated species with one set of parameters and identical constraints. Although we have not measured the deuterated phenol dimer, we can compare the changes in the rotational constants of our structure upon deuteration with the values obtained by Felker and co-workers. Table 5 lists the change of the distance R upon deuteration of the structure

TABLE 4: Summary of Experimental and Theoretical Results for Selected Internal Coordinates of the Phenol Dimer[a]

		structure I				ab initio			
	former RCS experiments[1]	S_0	S_1	$\Delta = X(S_1) - X(S_0)$[b]	semi-emp.[11]	MP2 6-31G(*d*)	B3LYP 6-31G(*d*)	HF 6-31G(*d*)	HF 6-31G(*d*,*p*)[2,10]
				Monomer center of mass distance [Å]					
R	5.273	5.255 ± 0.005	5.311 ± 0.04	+0.056 ± 0.045	5.232	5.097	5.854	6.005	5.993
				Rotational constants [MHz]					
A	1418.6	1414.4	1425.7	+10.6	1344.1	1366.4	1777.4	1844.8	1835.1
B	313.5	313.7	315.3	−6.7	318.0	325.6	251.6	240.8	241.8
C	285.5	287.5	275.3	−5.3	285.2	305.5	245.1	237.1	237.9
B + *C*	599.0	601.2	590.6	−12.0	603.2	631.1	496.7	477.9	479.7
				Intermolecular atom−atom distances [Å]					
O_1-O_2	3.00[c]	3.00[c]	2.96[c]	−0.04	3.05	2.88	2.87	2.96	2.97
C_8-H_2	2.93	2.92	2.59	−0.33	2.87	3.23	4.10	4.11	4.10
H_8-H_2	2.74	2.75	2.40	−0.35	2.64	3.11	3.73	3.72	3.71
				Intermolecular bond and dihedral angles [°]					
$\angle C_1O_1O_2$	108.8[c]	108.8[c]	108.8[c]		108.8	108.8	113.1	114.8	114.8
$\angle O_1O_2C_7$	117.8	117.1	131.4	+14.3	115.4	111.7	115.6	120.1	119.5
$\angle O_1O_2H_7$	131.6	132.1	113.6	−18.5	131.7	137.2	133.8	128.0	128.3
$\angle C_2C_1O_1O_2$	0.0[c]	0.0[c]	0.0[c]		−2.4	−7.8	−4.7	−1.8	−2.1
$\angle C_1O_1O_2C_7$	−59.2	−62.0	−29.7	+32.3	−56.4	−69.6	−110.1	−107.8	−107.5
$\angle O_1O_2C_7C_8$	−13.7	−13.9	−30.4	−16.5	−12.3	−12.3	−4.4	−5.3	−4.7
$\angle C_1O_1O_2H_7$	100.7	100.1	118.8	+18.7	112.0	93.0	80.3	84.0	83.6
				Alignment of the transition dipole moment (TM) [%]					
a	62.4	61.1	78.7		55.5	44.4	23.1	27.5	37.5
b	11.6	11.2	18.6		13.7	3.4	63.7	55.5	51.4
c	26.0	27.7	2.7		30.8	52.1	13.2	17.1	11.1
				Rotational constants of monomer (1) and monomer (2) [MHz]					
A(1)	5650.1	5650.1	5313.7	−336.4	5590.0	5644.2	5650.7	5751.5	5753.2
B(1)	2620.2	2620.2	2621.0	+0.8	2524.2	2608.7	2609.6	2656.1	2657.5
C(1)	1790.1	1790.1	1755.2	−34.9	1739.0	1784.1	1785.2	1817.0	1817.9
A(2)	5650.1	5650.1	5650.1	0.0	5590.0	5622.5	5632.5	5736.8	5738.9
B(2)	2620.2	2620.2	2620.2	0.0	2524.2	2612.7	2613.3	2657.2	2658.5
C(2)	1790.1	1790.1	1790.1	0.0	1739.0	1783.8	1785.1	1816.1	1816.9
				Dipole moment [Debye]					
μ					3.0	3.65	3.56	3.48	3.43

[a] Comparison of structures from the RCS results of Felker and co-workers,[1] ground and excited state RCS data of this work, semi-empirical calculations of Abdoul-Carime et al.,[11] and ab initio geometry optimization at the MP2, DFT/B3LYP, and HF levels of theory. [b] Difference between electronic excited state and ground state for parameter *X*. [c] Boundary condition.

TABLE 5: Changes in Center of Mass Distance (*R* [Å]) upon Deuteration of Structure (I) Compared with Former RCS Results[1]

	structure (I) S_0	structure from ref 1	calcd[a]
h_6-h_6	5.26	5.27	5.27
d_1-d_1	5.23	5.24	5.25
d_6-d_6	5.28	5.30	5.32
d_5-d_5	5.31	5.33	5.35

[a] Calculated from the rotational constants of ref 1 by applying equations 6−8.

depicted in Figure 4. After correction of the results by an offset of 0.02 Å, which is caused by the reported averaged structure of the S_0 and the S_1 state in ref 1, a good agreement with the *R* values obtained by Felker is achieved.

C. Structural Changes upon Electronic Excitation. Starting from the structure for the electronic ground state of the phenol dimer, we tried to evaluate possible changes upon electronic excitation of the donor moiety. The rotational constants from the excited state of phenol dimer have been extracted from the RCS results, and a center of mass (CM) distance of the monomer moieties of $R' = 5.31$ Å ± 0.04 Å has been calculated. Thus a small increase by +0.06 Å of this distance is obtained upon excitation. To evaluate the structure, there are again only three parameters determined from the experiment. Therefore, similar to the discussion of the structure in the ground state, a linear hydrogen bond and a decrease of the O_1-O_2 distance by 0.04 Å (as obtained for the phenol•water cluster upon electronic excitation[33]) have been assumed. Tables 4 and 6 show the structural changes obtained in this way. Again, those changes are only exemplary, because alternatively a change in the angles $\angle C_2C_1O_1O_2$ and $\angle C_1O_1O_2$ could be assumed. Moreover, those

TABLE 6: Comparison of Different Phenol Dimer Structures of the Ground State and Electronically Excited State

	structure (II) S_0	structure (II) S_1	structure (III) S_0
	Intermolecular atom−atom distances [Å]		
O_1-O_2	2.93[a]	2.89[a]	3.36
C_8-H_2	2.97	2.64	2.72
H_8-H_2	2.85	2.51	2.23
	Intermolecular bond and dihedral angles [°]		
$\angle C_1O_1O_2$	108.8[a]	108.8[a]	108.8[a]
$\angle O_1O_2C_7$	120.4	134.0	103.6
$\angle O_1O_2H_7$	127.7	108.7	147.5
$\angle C_2C_1O_1O_2$	0.0[a]	0.0[a]	0.0[a]
$\angle C_1O_1O_2C_7$	−59.6	−26.2	−69.1
$\angle O_1O_2C_7C_8$	−18.6	−37.1	−3.6
$\angle C_1O_1O_2H_7$	97.9	116.8	117.2
	Alignment of the transition dipole moment (TM) [%]		
a	62.9	79.4	53.4[a]
b	26.6	18.7	15.1
c	10.5	1.9	31.5

[a] Boundary condition.

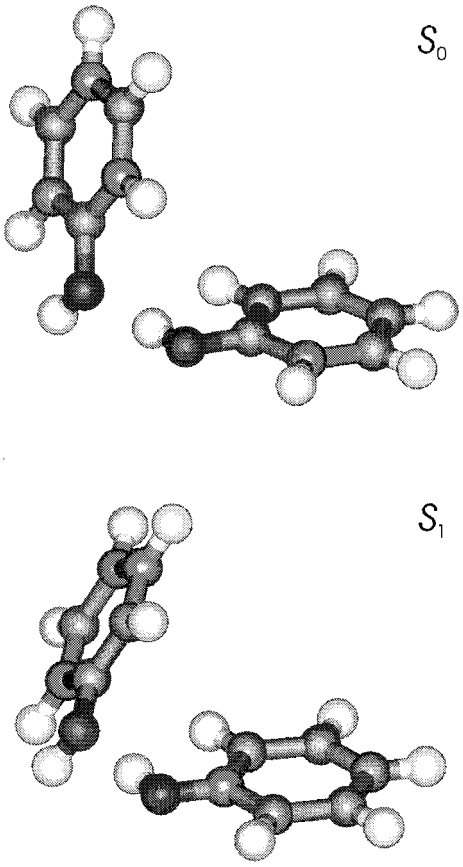

Figure 11. Structure (II) in the S_0 and structure (II) in the S_1 from Table 6.

changes are strongly affected by the choice of $(B - C)'$, which is only known with an uncertainty of 40% (see section IV.C). Depending on the choice of this parameter, nearly no structural changes or very strong changes between ground and electronically excited state structures can be obtained. Strong changes mainly consist of a decrease of the wagging angle of up to 40°. Two exemplary structures are depicted in Figure 11. Moreover, it has to be pointed out that the variability for this angle is not found for the CM distance R', which has been determined with 0.8% relative uncertainty. However, for the phenol dimer cation, recently a structure, similar to the ground-state structure, has been proposed. No sandwich-type structure such as that for other aromatic dimer cations could be confirmed.[42] Thus a large structural change is not very likely for the excited state of the phenol dimer.

VII. Structural Interpretation

In the following we will discuss some structural aspects of the phenol dimer in the ground-state based on the ab initio results. Moreover, a sensitivity analysis for the six intermolecular coordinates was performed, and a comparison with the experimental data will be presented.

The result of the ab initio calculation at the MP2/6-31G(*d*) level of theory will be considered as a reference structure (for the structure see also Figure 4). It agrees well with the result of the semiempirical calculation and with the experimental data of this work. The gross structure is also similar to the one reported by Felker and co-workers.[1] Both phenol rings are connected by an intermolecular hydrogen bond with an O−O (H···O) distance of 2.88 Å (1.92 Å), so that an acceptor and a donor phenol can be distinguished. The phenyl ring planes are not parallel but form an angle, here termed wagging angle $\angle C_1O_1O_2C_7$, of −69.6° at a center of mass distance of 5.10 Å. The molecular axis system (*a*, *b*, *c*) is located in the (inter)-molecular frame so that the *a* axis (prolate top axis) interconnects the center of masses of the individual phenol molecules. The phenol dimer is a nearly prolate top with an asymmetry factor of $\kappa'' = -0.96$. The *b* axis nearly bisects the angle between both long axes of the rings, whereas the *c* axis is nearly parallel to the aromatic planes. As a result of this geometry, the transition dipole moment of the donor moiety, which we assume to be fixed in the aromatic ring along the short axis, is of hybrid nature with the components 44.4% *a*, 3.4% *b*, and 52.1% *c*.[40] For the acceptor phenol, not investigated here, one would receive 43.2% *a*, 3.0% *b*, and 53.9% *c*.

The attractive interaction between the phenyl-moieties under the constraints imposed by the O−H···O hydrogen bond leads to a deviation from planarity of the angle $\angle C_2C_1O_1O_2 = -7.8°$. The oxygen atom O_2 is shifted from the plane of the donor moiety by 0.4 Å. In contrast, the in-plane bend angle $\angle C_1O_1O_2 = 108.8°$ corresponds to the typical value for a linear O−H···O hydrogen bond.

It is instructive to compare the donor and acceptor molecules in the energy-optimized dimer with the free monomer. Here we found upon dimerization an increase of the C−O bond length of +0.013 Å and the angle $\angle C_6C_1C_2$ of +1.0° for the acceptor molecule. This may be rationalized by the reduced charge density at the acceptor oxygen atom. Domenicano observed a correlation with the angle and the electronegativity of the substituent.[43] Here the electronegativity is increased by the hydrogen bonding. On the other hand the donor phenol molecule exhibits a slight shortening of the C−O and an increase of the O−H bond (−0.003 Å and +0.007 Å, respectively). Thus the hydrogen bond is well characterized by the calculation.

Information on the length of the hydrogen bond can be obtained by comparing the ab initio calculation and the experimental values for the phenol•water cluster. The O_1-O_2 distance has been derived from the experimental data to be 2.93(2) Å.[33] An ab initio calculation on the MP2/6-31G(*d*,*p*) level gives an O_1-O_2 distance of 2.845 Å, which is 0.085 Å too short.[38] It is likely, that a similar shortening of the O_1-O_2 hydrogen bond is produced by the MP2 calculations of the phenol dimer. Correcting its value leads to an expected O_1-O_2 distance of 2.95 Å for the phenol dimer.[44]

To characterize a molecular polyatomic dimer completely, six intermolecular coordinates are necessary as already mentioned. These coordinates are usually reflected in the low-frequency normal modes of the "supermolecule". Moreover, these modes represent large amplitude motions of the system, which can be considered as "soft coordinates" of the structure, so that a sensitivity analysis for the rotational constants with respect to these coordinates should reflect the quality of the proposed structure. For the sensitivity analysis, we performed one-dimensional model calculations starting from the optimized structure (I) with the intermolecular coordinates: wagging angle ($\angle C_1O_1O_2C_7 = -62.0°$), in-plane and out-of-plane twist angle ($\angle O_1O_2C_7C_8 = -13.9°$, $\angle O_1O_2C_7 = 117.1°$), in-plane and out-of-plane bend angle ($\angle C_1O_1O_2 = 108.8°$, $\angle C_2C_1O_1O_2 = 0.0°$), and O_1-O_2 distance = 3.0 Å. These intermolecular coordinates can be related to the intermolecular modes: butterfly (ν_1), mutual twisting (ν_2), cogwheel motion (ν_3), torsion (ν_4,ν_5), and hydrogen bond stretching (ν_6), respectively, as assigned by Kleinermanns et al.[2] Figure 12 shows the results of the sensitivity analysis. The value 1.0 on the *y*-axes indicates the experimental results. The position on the *x*-axes, which is indicated in each plot, marks the optimized structure (I), i.e.,

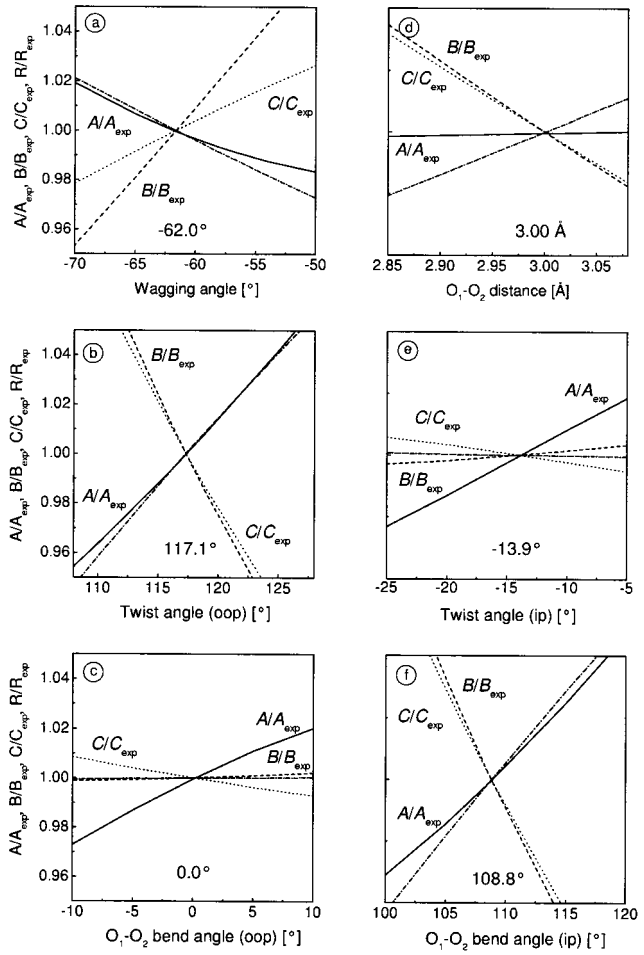

Figure 12. Sensitivity analysis of ground-state rotational constants and the center of mass distance *R* (dashed−dotted), based on the values for the S_0 structure (I) in Table 4. The dependence of the rotational constants on the following coordinates is shown: (a) wagging angle ∠ $C_1O_1O_2C_7$, (b) (oop) twist angle ∠ $O_1O_2C_7$, (c) O_1-O_2 bend angle (oop) ∠ $C_2C_1O_1O_2$, (d) O_1-O_2 distance, (e) (ip) twist angle ∠ $O_1O_2C_7C_8$, (f) O_1-O_2 bend angle (ip) ∠ $C_1O_1O_2$.

the starting structure (see also Table 4). Since a perfect fit has been obtained (six degrees of freedom determined from six parameters), all four graphs intersect at one point, which is determined by these two parameters. All diagrams of Figure 12 show a nearly linear relationship of the normalized rotational constants and the CM distance with respect to the intermolecular parameters. The individual slopes for *A*, *B*, *C*, and the CM distance *R* vary for the different intermolecular parameters. Also, for a fixed intermolecular parameter different slopes are obtained for *A*, *B*, *C*, and *R*. This illustrates that it is possible to change for example the wagging angle and retain the values for *A*, *B*, *C*, and *R* by adjusting the five remaining intermolecular parameters.

As can be seen from Figure 12, an increase of the O_1-O_2 distance leads to a decrease of the *B* and *C* rotational constants and an increase of *R*, whereas the *A* rotational constant is nearly unchanged. The suggested increase of the O_1-O_2 distance of 0.085 Å leads to a decrease of *B* and *C* of about 2% and an increase of *R* of about 1%. Those three values from the MP2 *ab initio* calculation are therefore shifted closer to the experimental values of the phenol dimer (see Table 4). This discussion should be understood qualitatively, since this simple picture does not take into account a relaxation of the other intermolecular parameters. However, these results suggest, that the theoretical description of the phenol dimer in the electronic ground state could be further improved by ab initio calculations, which give a more accurate description of the hydrogen bond and incorporate the dispersive interaction of the aromatic rings.

Although t_H' and t_J' have been determined with high accuracy, the difference between the B' and the C' rotational constants has been determined only with a limited accuracy (40% relative uncertainty, in comparison with 4% for the ground state). This is due to the fact that no excited-state C'-type transients have been allocated in the TRFD spectrum, as discussed in section V.C. This uncertainty leads to a range of possible dimer structures for the electronically excited state, as discussed in section VI.C. The wagging angle has been found in the range from −60° (nearly no change) to −20°. Although the precise values are not known, such a change could be rationalized by an increased interaction of the phenyl rings. In summary, the precise elucidation of the structural changes upon electronic excitation of the phenol dimer have to await accurate values for all three excited-state rotational constants and a high level ab initio calculation for the electronically excited state.

VIII. Conclusion

We reported on a high-resolution rotational coherence spectroscopy (RCS) investigation of the phenol dimer, applying the TRFD method. The resolution was sufficient to resolve ground state and electronically excited-state transients upon photoexcitation of the 0_0^0 transition in the phenol donor moiety. The assignments of the excited state *J*-type transients were verified by a $(1 + 1')$ pump−probe ionization (PPI) experiment. The *H*-type transients were assigned by comparing numerical simulations with the experimental TRFD spectrum. By using a search and fit routine, values for the rotational constants of the ground state and the electronically excited state of the phenol dimer and their error margins were obtained. The estimated uncertainties of the rotational constants of the electronic ground state are 0.04%, 0.3%, and 0.2% for the *A*, *B*, and *C* constants, respectively. Higher uncertainties are obtained for the rotational constants of the electronically excited state (0.2%, 2.5%, and 2.5%). The rotational constants of the phenol dimer in the S_1 excited state have been reported for the first time. The averaged values of the ground state and excited-state rotational constants of this work are in good agreement with former RCS results obtained with a lower time resolution.[1]

We propose possible structures of the phenol dimer in both, the electronic ground and excited state as obtained by a fitting procedure, using the experimentally determined rotational constants and constraints imposed by the O−H···O hydrogen bond. For the electronic ground state the results are in a good agreement with both semiempirical calculations[11] and ab initio calculations at the MP2/6-31G(*d*) level of theory. Upon electronic excitation, only small changes of the rotational constants have been found. From that, a slight increase in the center of mass distance by 0.06 Å was obtained. Since the uncertainty of $(B - C)'$ in this investigation is still large (≈40%), we cannot rule out a larger change of the structure, e.g., a decrease of the wagging angle by several tens of degrees, which would lead to a more pronounced "facing" of the aromatic rings. To pinpoint the electronically excited-state structure clearly, the difference between B' and C' has to be determined more accurately. This could be achieved with excited-state selective RCS methods in order to record C'-type transients at long time delays. However, the excited-state rotational constants obtained here are useful to check high-level ab initio calculations. It should be added that precise experimental data on the rotational constants of the electronically excited states of dimers of aromatic molecules are still rare.

Acknowledgment. Dedicated to Prof. E. W. Schlag on the occasion of his 68th birthday. We are thankful to M. Schmitt (Universität Düsseldorf) for pointing out the problem of the phenol dimer structure. We thank Peter M. Felker (UCLA) for supply with the computer code for numerical RCS simulations. We gratefully acknowledge funding from the Adolf-Messer-, Hermann-Willkomm-, Bodo-Sponholz-Stiftung, and the Fonds der Chemischen Industrie. The Deutsche Forschungsgemeinschaft (DFG) and the Johann Wolfgang Goethe-Universität Frankfurt/M. are acknowledged for their generous financial support.

References and Notes

(1) Connell, L. L.; Ohline, S. M.; Joireman, P. W.; Corcoran, T. C.; Felker, P. M. *J. Chem. Phys.* **1992**, *96*, 2585.

(2) Kleinermanns, K.; Gerhards, M.; Schmitt, M. *Ber. Bunsen-Ges. Phys. Chem.* **1997**, *101*, 1785.

(3) Fuke, K.; Kaya, K. *Chem. Phys. Lett.* **1982**, *91*, 311.

(4) Fuke K.; Kaya, K. *Chem. Phys. Lett.* **1983**, *83*, 97.

(5) Hartland, G. V.; Henson, B. F.; Venturo, V. A.; Felker, P. M. *J. Phys. Chem.* **1992**, *96*, 1164.

(6) Dopfer, O.; Lembach, G.; Wright, T. G.; Müller-Dethlefs, K. *J. Chem. Phys.* **1993**, *98*, 1933.

(7) Sur, A.; Johnson, P. M. *J. Chem. Phys.* **1986**, *84*, 1206.

(8) Ebata, T.; Watanabe, T.; Mikami, N. *J. Phys. Chem.* **1995**, *99*, 5761.

(9) Schmitt, M.; Henrichs, U.; Müller, H.; Kleinermanns, K. *J. Chem. Phys.* **1995**, *103*, 9918.

(10) Kleinermanns, K.; Gerhards, M.; Schmitt, M. http://www-public.rz.uni-duesseldorf.de/~pc1/abinitio/, phenol dimer, 1997.

(11) Abdoul-Carime, H.; Wakisaka, A.; Flugge, J.; Takeo, H.; Periquet, V.; Schermann, J. P.; Desfrançois, C. *J. Chem. Soc., Faraday Trans.* **1997**, *93*, 4289.

(12) Felker, P. M. *J. Phys. Chem.* **1992**, *96*, 7844.

(13) Felker, P. M.; Zewail, A. H. In *Femtochemistry*; Manz, J., Wöste, L., Eds.; VCH: Weinheim, 1995; Vol. I, Chapter 5.

(14) Riehn, C.; Weichert, A.; Lommatzsch, U.; Zimmermann, M.; Brutschy, B. *J. Chem. Phys.* **2000**, *112*, 3650.

(15) Weichert, A.; Riehn, C.; Brutschy, B. *J. Chem. Phys.* **2000**, *113*, 7830.

(16) Riehn C.; Weichert, A.; Brutschy, B. *Phys. Chem. Chem. Phys.* **2000**, *2*, 1873.

(17) Weichert, A.; Riehn, C.; Barth, H.-D.; Lembach, G., Zimmermann, M.; Brutschy, B.; Podėnas, D. *Rev. Sci. Instrum.*, accepted for publication.

(18) The terms positive and negative polarity are used with reference to a time-resolved fluorescence depletion experiment (TRFD).

(19) GAUSSIAN 94, Revision E.3, and Revision D.4, Frisch, M. J.; Trucks, G. W.; Schlegel, H. B.; Gill, P. M. W.; Johnson, B. G.; Robb, M. A.; Cheeseman, J. R.; Keith, T.; Petersson, G. A.; Montgomery, J. A.; Raghavachari, K.; Al-Laham, M. A.; Zakrzewski, V. G.; Ortiz, J. V.; Foresman, J. B.; Cioslowski, J.; Stefanov, B. B.; Nanayakkara, A.; Challacombe, M.; Peng, C. Y.; Ayala, P. Y.; Chen, W.; Wong, M. W.; Andres, J. L.; Replogle, E. S.; Gomperts, R.; Martin, R. L.; Fox, D. J.; Binkley, J. S.; Defrees, D. J.; Baker, J.; Stewart, J. P.; Head-Gordon, M.; Gonzalez, C.; Pople, J. A., Gaussian, Inc., Pittsburgh, PA, **1995**.

(20) Benharash, P.; Gleason, M.; Felker, P. M. *J. Phys. Chem. A* **1999**, *103*, 1442.

(21) Gonzalez, C.; Lim, E. *J. Phys. Chem. A* **1999**, *103*, 1437.

(22) Note that the (1 + 1′) PPI trace in ref 16 has been accidentally reproduced with the wrong polarity and has therefore to be inverted.

(23) Unpublished results.

(24) Riehn, C.; Weichert, A.; Zimmermann, M.; Brutschy, B. *Chem. Phys. Lett.* **1999**, *299*, 103.

(25) Computer code for numerical RCS simulations, courtesy of P. M. Felker (UCLA).

(26) Press, W. H.; Teukolsky, S. A.; Vetterling, W. T.; Flannery, B. P. *Numerical Recipes in FORTRAN. The Art of Scientific Computing*, 2nd ed.; Cambridge University Press: Cambridge, 1992.

(27) Assuming only normally distributed noise components on the RCS signal, it would be possible to calculate a $\Delta\chi^2$ corresponding to the desired level of confidence (e.g., 95%). This assumption is not justified in our case because of not normal-distributed noise components on the RCS signal, e.g., those caused by saturation effects, and the high-pass-filtering method used to prepare the data. One would have to use results of a detailed modeling of the signal generation process or Monte Carlo simulations to determine the correct $\Delta\chi^2$ contour for the desired confidence level. This has not been done so far, but it is nevertheless possible to conservatively estimate a $\Delta\chi^2$ contour which should correspond to a high level of confidence ($>$ 95%). Hence, we use $\Delta\chi^2/\chi^2_{min} = 2\%$. The resulting error margins are in good agreement with the values obtained by the linear regression approach.

(28) The same direction of the transition dipole moment for the pump and the probe pulse has been assumed.

(29) Larsen, N. W. *J. Mol. Struct.* **1979**, *51*, 175.

(30) Kraitchman, J. *Am. J. Phys.* **1953**, *21*, 17.

(31) Christoffersen, J.; Hollas, J. M.; Kirby, G. H. *Proc. R. Soc. A* **1968**, *307*, 97.

(32) Hollas, J. M. *J. Chem. Soc., Faraday Trans.* **1998**, *94*, 1527.

(33) Berden, G.; Meerts, W. L.; Schmitt, M.; Kleinermanns, K. *J. Chem. Phys.* **1996**, *104*, 972.

(34) Zarodnik, V. E.; Bel'skii, V. K.; Zorkii, P. M. *Zh. Strukt. Khim.* **1987**, *28*, 175.

(35) Portalone, G.; Schultz, G.; Domenicano, A.; Hargittai, I. *Chem. Phys. Lett.* **1992**, *197*, 482.

(36) Lampert, H.; Mikenda, W.; Karpfen, A. *J. Phys. Chem. A* **1997**, *101*, 2254.

(37) Michalska, D.; Bieńko, D. C.; Abkowicz-Bieńko, A. J. *J. Phys. Chem.* **1996**, *100*, 17786.

(38) Fang, W.-H. *J. Chem. Phys.* **2000**, *112*, 1204.

(39) Roth, W.; Imhof, P.; Gerhards M.; Schumm, S.; Kleinermanns, K. *Chem. Phys.* **2000**, *252*, 247.

(40) The alignment of the transition dipole moment (TM) has been assumed parallel to the C_2-C_6 axis of the donor moiety.

(41) Cvitaš, T.; Hollas, J. M.; Kirby, G. H. *Mol. Phys.* **1970**, *19*, 305.

(42) Ohashi, K.; Inokuchi, Y.; Nishi, N. *Chem. Phys. Lett.* **1996**, *257*, 137.

(43) Domenicano, A. In *Accurate Molecular Structures*; Domenicano, A., Hargittai, I., Eds.; Oxford University Press: Oxford, 1992; Chapter 18.

(44) Based on a calculated O_1-O_2 distance of 2.864 Å, which has been obtained from an MP2/6-31G(*d*,*p*) ab initio calculation of the phenol dimer.